Original Article
Food Science and Technology

ISSN 0101-2061 (Print)
ISSN 1678-457X (Online)

DOI: https://doi.org/10.1590/fst.119421

Characterisation and antioxidant activity of polysaccharide iron (III) complex in Qingzhuan Dark Tea

Hongfu ZHOU[1#], Ziyao WANG[1#], Huimin MA[1], Shiyue WANG[1], Wenjing XIE[1], Yong CHEN[1], Chen XIE[1], Anran GUO[1], Cai WANG[1*], Min ZHENG[1*]

Abstract

Anaemia, caused by iron deficiency, is a common disease in some parts of the world. A traditional medicine for treating anaemia resulting from iron deficiency is inorganic iron, which is represented by ferrous sulfate. However, serious irritation to the gastrointestinal tract is one of the side effects caused by inorganic iron. We extracted the tea polysaccharide (TPS) from Qingzhuan Dark Tea and employed a green technology to prepare a polysaccharide–iron [TPS-Fe(III)] complex. We further characterised the structure through thermogravimetric analysis, molecular weight analysis, atomic absorption spectroscopy, Fourier-transform infrared spectroscopy, ultraviolet spectroscopy (UV), ^{1}H nuclear magnetic resonance spectroscopy, scanning electron microscopy, X-ray diffraction analysis, X-ray photoelectron spectroscopy, and atomic mechanics microscopy. We performed a comparative evaluation of the antioxidant properties of the TPS-Fe(III) complex and TPS. The results indicated that the antioxidant activity of the TPS-Fe(III) complex is superior to that of TPS. The scavenging activity was determined using 2,2-diphenyl-1-picrylhydrazyl, hydroxyl, superoxide anion, and 2,2'-azobis-(3-ethylbenzothiazoline-6-sulfonic acid) radical scavenging activity assays and malondialdehyde inhibition assay. The structure of the TPS-Fe(III) complex formed by the complexation of the tea polysaccharide with iron ions was highly stable, which significantly improved its antioxidant activity in vitro. Thus, the TPS-Fe (III) complex can provide additional health benefits compared with other typical non-antioxidant iron nutritional supplements.

Keywords: Qingzhuan Dark Tea; polysaccharides; iron(III) complex; structural characterisation; antioxidant activity.

Practical Application: Develop Qingzhuan Dark Tea for pharmaceutical industry.

1 Introduction

Qingzhuan Dark Tea belongs to one of the six categories of tea and is produced primarily in Chibi city, Hubei Province, China. It is a life necessity for ethnic minorities in Northwest China under resource-limited conditions. Qingzhuan Dark Tea contains many active substances and has a wide range of biological activities (Feng et al., 2020). Qingzhuan Dark Tea activates fluid production and quenches thirst. Additionally, the tea is refreshing, aids in digestion and sterilisation, and treats diarrhoea. The tea can also help control hypertension, hyperlipidemia, and hyperglycemia.

The tea resources are abundant in China (Gao et al., 2021; Yao et al., 2021). Tea polysaccharide (TPS) serves as an antioxidant, anticoagulant, and antitumour agent; it lowers blood fat, blood pressure, and blood sugar and enhances immunity, thereby exhibiting a broad range of biological activities (Liu et al., 2016) . TPS appears mainly as a yellowish powder with good water solubility and is insoluble in high concentrations of ethanol, acetone diethyl ether, and other organic reagents. TPS is a natural macromolecular active substance that is present in a large amount in tea and has many biological activities. It was reported to exhibit a significant antioxidant capacity and effective scavenging activity against free radicals (Yang et al., 2017). Therefore, we believe that the polysaccharides and complexes of Qingzhuan Dark Tea exhibit a superior antioxidant capacity. In recent years, plenty of studies have been conducted on the application of TPS in the food industry, medical treatment, health care products, and skincare products to ensure appropriate use of the resources of all aspects of tea and promote its economic distribution. Qingzhuan Dark Tea consumption can also improve people's standard of living and advocate a healthy lifestyle.

Iron is a crucial trace element in the human body and plays an extremely vital role in body metabolism. It can affect the immune function of the body to some extent. It is an indispensable substance that maintains various normal physiological processes and plays a key role in the human body (Abualhasan et al., 2021). Iron is present in human tissues and organs mainly in two forms, namely functional iron and stored iron. The majority of the iron is stored in the body as functional iron, which binds to proteins in the blood and muscles and is involved in oxygen transport in the body.

TPS-Fe(III) complex is superior to inorganic iron supplements such as ferrous sulfate because of its minimal side effects on

Received 05 Nov., 2021
Accepted 27 Dec., 2021
[1] *Xianning Medical College, Hubei University of Science and Technology, Xianning, Hubei, China*
*Corresponding author: xyzhengmin@hbust.edu.cn
#These authors have contributed equally to this work.

the gastrointestinal digestive system, good stability, and high bioavailability (Raja et al., 2000) .TPS-Fe(III) complex is a brown powder, which is insoluble in methanol, ethanol, ether, and other organic solvents but soluble in water. It does not release free iron in the aqueous solution and exhibits no sedimentation and hydrolysis but high stability. Polysaccharides, as ligands, form surface complexes on the nuclear surface, which belong to polymer compounds. TPS-Fe(III) is a complex of polysaccharides and iron, and it does not contain free Fe^{2+} and Fe^{3+}. It is easy to be assimilated and absorbed by the body. It has strong reducibility and can be reduced to bivalent iron for absorption. TPS-Fe(III) can promote the body's haematopoietic function, rapidly improve the level of haemoglobin, and effectively treat and prevent anaemia caused by iron deficiency (Tveden-Nyborg et al., 2021).

Thus, considering TPS-Fe(III) as a type of iron supplement worthy of further research and development, the present study aims to perform the structural characterisation and investigate the antioxidant activity of TPS-Fe(III). In this study, the structural characterisation and physical properties of TPS-Fe(III) were analysed by thermogravimetric analysis (TGA), molecular weight analysis, atomic absorption spectroscopy (AAS), Fourier-transform infrared spectroscopy (FTIR), ultraviolet (UV) spectroscopy, ^{1}H nuclear magnetic resonance (1H NMR) spectroscopy, scanning electron microscopy (SEM), X-ray diffraction (XRD) analysis, X-ray photoelectron spectroscopy (XPS), and atomic mechanics microscopy (AFM). Additionally, a series of *in vitro* experiments was conducted to determine the antioxidant activity of the TPS-Fe(III) complex.

2 Materials and methods

2.1 Experimental materials

The Qingzhuan Dark Tea was obtained from Chibi city, Hubei Province, China. Iron citrate (AR), 2,2-diphenyl-1-picrylhydrazyl, hydroxyl (DPPH), and 2,2'-azobis-3-ethylbenzothiazoline-6-sulfonic acid (ABTS) were procured from McLean (China). All reactants were used, unless otherwise specified, in this study. Deionised water was used for all experiments.

2.2 Preparation of TPS

The tea powder was extracted using water for 4 h after degreasing and removing the small molecules. The supernatant was lyophilised to obtain crude polysaccharides. First, 50 g of polyamide was soaked in 95% ethanol, 5% NaOH, and 10% hydrochloric acid for 4–5 h,respectively. Then, the polyamide resin was loaded into the column. The polyamide column was balanced after natural settlement, and TPS was dissolved in water. Further, the TPS was subjected to elution, decolorisation, and deproteinisation to obtain the eluent. The refined polysaccharides were freeze-dried after 48 h of dialysis. The content of sugar in refined polysaccharides was determined using the phenol-concentrated sulfuric acid method at 490 nm.

2.3 Preparation of the TPS-Fe(III) complex

Briefly, 0.1 g of TPS was weighed and placed in a 50-mL conical flask containing a constant volume of deionised water. TPS was placed in a water bath at 60 °C and shaken continuously until it was completely dissolved. TPS was mixed with an equal volume of 0.05% iron citrate solution in a magnetic agitator at 60 °C for 2 h and then cooled to room temperature. Then, four times the 80% ethyl alcohol volume was added to the mixture and incubated overnight. The TPS-Fe(III) complex of Qingzhuan Dark Tea was obtained after 48 h of dialysis and freeze-drying.

2.4 Physical and chemical properties of the TPS-Fe(III) complex and iron ion identification reaction

To determine the solubility of Qingzhuan Dark Tea TPS-Fe(III) in different solutions, 10 g of the Qingzhuan Dark Tea polysaccharides and TPS-Fe(III) complex were weighed first. Then, 5 mL of deionised water and 5 mL of 1 mol/L hydrochloric acid were added to obtain a corresponding water solution of 1 mg/mL and a hydrochloric acid solution of 1 mg/mL. Further, 10% potassium ferrocyanide and potassium thiocyanate solution were added to the prepared aqueous solution and hydrochloric acid solution. Then, the changes in each solution after the addition of the reagent were observed and recorded.

2.5 Structure characterisation of TPS and TPS-Fe(III)

The thermogravimetry analysis (TGA) was performed using the NETZSCH thermogravimetric analyzer (TG 209F3, Germany) under N_2 atmosphere with a heating rate of 10 °C/min and at an ambient temperature of 600 °C.

The relative molecular weight and homogeneity of TPS and TPS-Fe(III) were determined through high-performance gel filtration chromatography (HPGPC). Two milligram each of TPS and TPS-Fe(III) complex were weighed and dissolved in 400 μL and 0.1 mol/L sodium nitrate solution, respectively, to determine the homogeneity and molecular weight distribution of TPS and TPS-Fe(III) complex. The mobile phase used was 0.1 mol/L sodium nitrate solution, with a 0.9 mL/min flow rate and a column temperature of 45 °C.

An atomic absorption spectrometer (CONTRA A-700) was used to conduct a single element quantitative analysis (flame method) for the qualitative and quantitative analyses of iron in the TPS-Fe(III) complex.

FTIR and 1H NMR analyses of both TPS and TPS-Fe(III) complex were used to detect the structural changes caused by iron complexation. The organic functional groups in TPS and TPS-Fe(III) complex were categorised by infrared spectroscopy. Specifically, the samples were ground with potassium bromide powder and pressed into 1-mm flakes. The FTIR measurements were then conducted using a Nicolet 6700 Fourier-transform infrared spectrophotometer in the frequency range of 4000–400 cm^{-1} (Iwansyah et al., 2021). The samples acquired in D_2O with chemical shifts are expressed as δ PPM. The ^{1}H NMR spectroscopic analysis involved 8 scans at 25 °C using a Bruker 400 MHz NMR at room temperature. The spectra were processed using Mestre Nova 6.1.1.

TPS and the TPS-Fe(III) complex were prepared into 0.5 mg/mL solution and added into a quartz colorimetric dish. Further,

the UV spectrum was scanned with a spectrophotometer in the 200–400 nm range.

The surface morphology and structure of TPS and the TPS-Fe(III) complex were examined and observed using a field emission scanning electron microscope (Zeiss Ultra Plus) with 5 kV acceleration voltage. Simultaneously, the surface element composition between TPS and the TPS-Fe(III) complex was compared by EDS. TPS and TPS-Fe(III) crystal structures were categorised using an Empyrean X-ray diffractometer (Panaco, The Netherlands).

An X-ray photoelectron spectrometer (Escalab 250XI, USA) was used to determine the iron valence states in the TPS-Fe(III) complex and the binding energy before and after the reaction.

The morphology of TPS and TPS-Fe(III) complexes was studied using the atomic force microscope (AFM) Nanoscope IV (Veeco, USA). TPS and TPS-Fe(III) solutions (10 μg/mL) were precipitated on the newly cut surface and allowed to dry in air for approximately 10 min. Two-micrometre images were processed and examined using Gwyddion-SPM data analysis software.

2.6 Antioxidant test

The research method was used for analysis, with slight modifications (Akram et al., 2017; Liu & Li, 2021) . Six test tubes were taken, and 1 mL of different concentrations of TPS and TPS-Fe(III) (0.0, 0.2, 0.4, 0.6, 0.8, 1.0 mg/mL) were added to each tube. Further, 0.2 mmol/L of DPPH-methanol solution (1 mL) was added to each test tube, and the mixture was mixed thoroughly. The mixture was incubated at 30 °C in the dark for 30 min to avoid the light reaction, and the absorbance was measured at 518 nm.

$$DPPH\ free\ radical\ scavenging\ rate\ (\%) = \left[1-(A_1-A_2)/A_0\right] \times 100\% \quad (1)$$

Here (Equation 1), A_1 is the absorbance of the sample solution with DPPH, A_0 is the absorbance without sample solution, and A_2 is the absorbance without DPPH solution. The clearance rate was calculated separately. Six parallel measurements were made, and the average values were considered.

The hydroxyl radical scavenging activity was determined through spectrophotometry. The method was used with slight modifications (Yang et al., 2020). To the six test tubes, 1.5 mL of 7.5 mol/L ferrous sulfate solution and 3 mL of 8 mmol/L salicylic acid-ethanol solution were added. Further, 1.5 mL of TPS and TPS-Fe(III) solutions with different concentrations (0.0, 0.2, 0.4, 0.6, 0.8, 1.0 mg/mL) were added. Finally, 3 mL of 7.5 mmol/L hydrogen peroxide solution was added, which was fully mixed and incubated for 45 min at 37 °C. The absorbance was determined at 510 nm (A_1). According to aforementioned operation, the solution without sample was taken as A_0, and the clearance rate was calculated (Equation 2).

$$Hydroxyl\ radical\ scavenging\ rate\ (\%) = (A_0-A_1)/A_0 \times 100\% \quad (2)$$

The research method was used with a minor modification (Guo et al., 2014). Six test tubes were taken, and 1 mL of different concentrations of TPS and TPS-Fe(III) (0.0, 0.2, 0.4, 0.6, 0.8, 1.0 mg/mL) were added to each of them. Further, 5 mL of 0.05 mol/L Tris-HCl buffer with a pH value of 8.2 was added to each tube and then thoroughly mixed. The reaction was left standing for 10 min in a water bath at 25 °C. Then, 0.4 mL of 30 mmol/L catechol solution was added under the same conditions for 4 min, and the reaction was terminated with 8 mol/L HCl. The absorbance value was determined at 320 nm.

$$Superoxide\ anion\ radical\ scavenging\ rate\ (\%) = (A_0-A_1)/A_0 \times 100\% \quad (3)$$

where A_1 is the absorbance of the sample solution at 320 nm, A_0 is the absorbance without sample solution (Equation 3). The clearance rate was calculated separately. Six parallel measurements were made, and the average values were considered.

The ABTS radical scavenging activity of the TPS-Fe(III) complex was determined using the method described (Wang et al., 2021; Byun et al., 2021; Hu et al., 2021), with minor modifications. ABTS (0.3841 g) and potassium persulfate (0.0662 g) were accurately weighed and then dissolved in 20 mL deionised water. The reaction mixture was placed in a dark room at room temperature for 12–16 h before use. The resulting solution was diluted with phosphate-buffered saline (PBS) of pH 7.4 to a suitable concentration for use. Deionised water was used to prepare TPS and TPS-Fe(III) complex solutions with concentration gradients of 0, 0.2, 0.4, 0.6, 0.8, and 1.0 mg/mL. Then, 0.2 mL of the above gradient solutions was taken and mixed with 0.8 mL ABTS. The mixture was shaken well and placed in the dark at room temperature for 6 min.

$$ABTS\ free\ radical\ scavenging\ rate\ (\%) = \left[(A_0-A_1)/A_0\right] \times 100\% \quad (4)$$

where A_1 is the absorbance of the sample solution at 734 nm, and A_0 is the absorbance of the blank control (Equation 4). The clearance rate was calculated separately. Six parallel measurements were taken, and the average values were considered

The method (Zhang et al., 2021; Li et al., 2020) with slight modifications was used for the lipid peroxidation inhibition test of the TPS-Fe(III) complex. The rat liver was dissected at 4 °C, cleaned quickly, homogenised in 10 times the volume (v/w) of PBS, and diluted 25 times. TPS and TPS-Fe(III) complex solutions with concentration gradients of 0.0, 0.2, 0.4, 0.6, 0.8, and 1.0 mg/mL were prepared. Subsequenntly, 0.2 mL of the aforementioned gradient solutions were added to 0.1 mL of 6 mM ferrous sulfate, 0.05 mL of 3% hydrogen peroxide, and 1 mL of liver homogenate. The solution was then taken out, to which 1 mL of 10% TCA and 1 mL of 0.67% thiobarbituric acid (TBA) were added. Then, the solution was mixed and boiled for 15 min and immediately placed into the ice–water mixture for cooling. The supernatant was centrifuged at 4000 rpm for 20 min, and the absorbance was measured at 532 nm. The sample was replaced with deionised water and used as blank control.

$$Liver\ lipid\ peroxidation\ inhibition\ rate\ (\%) = \left[(A_0-A_1)/A_0\right] \times 100\% \quad (5)$$

where A_1 is the absorbance of the sample solution at 532 nm, and A_0 is the absorbance of the blank control. The clearance rate was calculated separately (Equation 5). Six parallel measurements were taken, and the average values were considered.

2.7 Statistical analysis

All results are expressed as mean ± standard deviation of six measured values. Statistical analysis was conducted using Origin 2019 software (Origin Lab Corporation, Northampton, MA, USA). One-way analysis of variance was performed using SPSS (version 18.0, IBM, Armonk, New York, USA). A P value of < 0.05 was considered statistically significant.

3 Results and discussion

3.1 Physicochemical properties of the TPS-Fe(III) complex and iron ion identification reaction

General properties of the TPS-Fe(III) complex: TPS-Fe(III) complex is odourless, tasteless, and highly water soluble. However, it does not dissolve easily in anhydrous ethanol, anhydrous methanol, ether, and other organic solvents. The chemical bond between polysaccharides and iron elements is disrupted by the action of strong acid. Consequently, the free iron ion shows its characteristic qualitative discrimination response. The solution did not show any change when potassium ferrocyanide and potassium thiocyanate were added to the aqueous solution of the TPS-Fe(III) complex. The hydrochloric acid solution of the TPS-Fe(III) complex was mixed with potassium ferrocyanide and potassium thiocyanate reagent.

Further, the ferrous potassium cyanide reagent solution was added until it appeared blue, and potassium thiocyanate reagent solution was added until it appeared dark red. The results indicated that the TPS-Fe(III) complex samples did not contain free iron ions, suggesting that the polysaccharides bind to iron rather than mixing physically with iron.

3.2 Determination of the TPS content and iron content of the TPS-Fe(III) complex

The content of total polysaccharides determined using the phenol sulfuric acid method was found to be 64.96%. The iron content measured using an atomic absorption spectrometer was 0.89%.

3.3 Thermal property analysis

TGA analysis was conducted to determine the extent of thermal weight loss of TPS and the TPS-Fe(III) complex; the results are displayed in Figure 1. The water bound to the polysaccharides chain evaporates at a temperature < 200 °C, and the degradation of the carbon chain occurs between 200 °C and 400 °C. Compared with TPS, the TPS-Fe(III) complex lost less total weight, probably due to the cross-linking reaction between polysaccharides and iron. In the process of complex formation, the spatial structure of the unstable system is changed to form a steady-state system (Dong et al., 2017). The preferred spatial approach is that the anionic groups can be stacked around

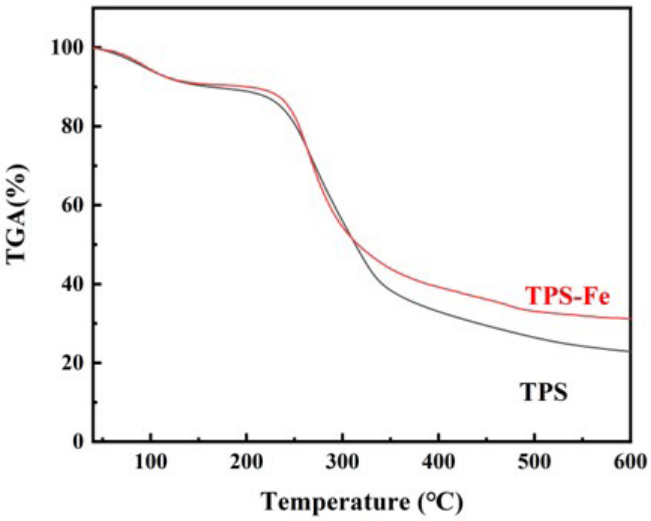

Figure 1. TGA curves for TPS and TPS-Fe(III).

the cation, and the size of the hole in which the cation resides affects the complex stability. Each ligand contains many donor groups and adopts the most favourable conformation in the complexation process. The introduction of iron ions increases the intramolecular and intermolecular binding and stability of the complex. Hence, the thermal stability of polysaccharides is boosted by adding iron, and the prepared TPS-Fe(III) complex is stable.

3.4 Molecular weight analysis

The mass average molecular weight (Mw), number average molecular weight (Mn), and polydispersity (Mw/Mn) of TPS and the TPS-Fe(III) complex were determined to assess the molecular structure and relative molecular weight of the combination of iron and polysaccharides. The molecular weight distribution was analysed through HPGPC, and the representative graph is shown in Figure 2. The TPS-Fe(III) complex (B) exhibited higher molecular weight and polydispersity (Mw: 22698 g/mol, Mw/Mn3.08) than TPS (A) (Mw:18458 g/mol. Mw/Mn: 2.86). The difference in the molecular weight may be attributed to the incorporation of iron into the main chain of polysaccharides, which may play a key role in controlling the molecular weight (Feng & Zhang, 2020) . Additionally, the molecular weight distribution curve showed the differences in the structural characteristics of TPS and the TPS-Fe(III) complex. Both TPS and the TPS-Fe(III) complex were found to exhibit the unimodal molecular weight distribution, indicating that the TPS was homogeneous and the formation of TPS-Fe(III) did not cause chain damage.

3.5 Infrared spectral analysis

To determine the structural differences between TPS and the TPS-Fe(III) complex, their FTIR spectra were recorded (Figure 3). An extensive intermolecular H-bonding network is present between all OH groups of the polysaccharides that holds the polymeric units together. This is consistent with the major broadening of the OH stretching vibrations in the region

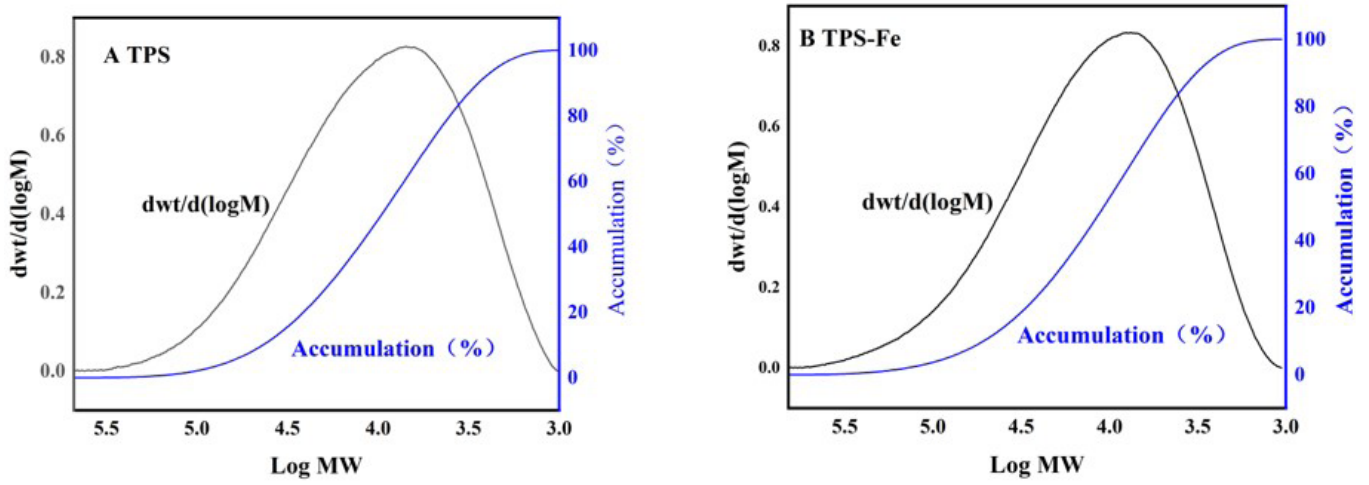

Figure 2. Relative molecular weight of TPS (A) and the TPS-Fe(III) complex (B).

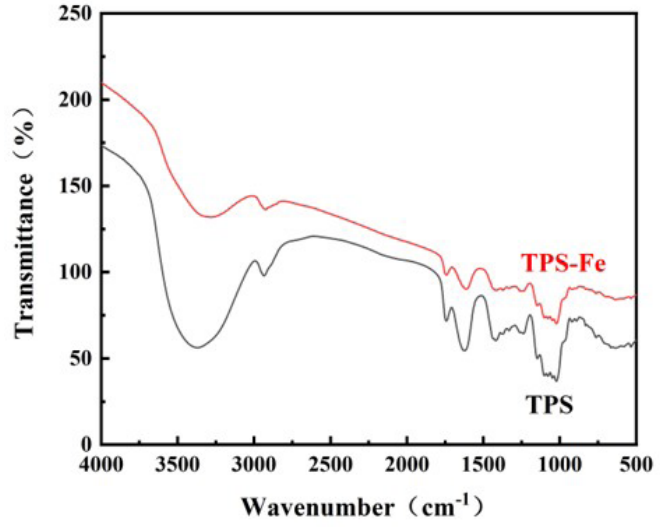

Figure 3. FTIR spectra of TPS and the TPS-Fe(III) complex.

of 3500–3200 cm^{-1} of TPS and the corresponding TPS-Fe(III) complex analysed in the present study. FTIR spectra display typical broad stretching peaks; a stretching peak of approximately 3375 cm^{-1} represents hydroxyl groups, and a stretching peak of approximately 2935 cm^{-1} corresponds to C-H stretching. The peak intensity at approximately 3375 cm^{-1} on the TPS-Fe(III) complex was weakened and shifted, which signified that the OH group was associated with iron. The coordination reaction of the iron ion with the hydroxyl oxygen atom resulted in the fading of the ability of the hydroxyl group to form intermolecular and intermolecular hydrogen bonds. The C-H tensile vibration also exhibited weakened strength after addition of iron, primarily due to the rearrangement of the hydrogen bond network of polysaccharides. Likewise, in the TPS-Fe(III) complex, the intensity of the associated peak at 1615 cm^{-1} represented the carbonyl group, where the power of the infrared absorption peak was weakened and exhibited a redshift compared with TPS (Liu et al., 2019), signifying the involvement of polysaccharides and iron in the complex reaction.

3.6 Ultraviolet spectrum analysis

UV–visible spectrum is a type of absorption spectrum, in which molecules absorb electromagnetic waves in the UV–visible region. Hence, UV–Vis spectroscopy can be used as an auxiliary tool for the structural analysis of compounds. UV–Vis spectroscopy is generally used to determine the coordination reaction and the change of ligand structure. The UV–Vis spectra of TPS and the TPS-Fe(III) complex are displayed in Figure 4. TPS and the TPS-Fe(III) complex no typical absorption peaks at 260 nm and 280 nm, respectively, due to a lack of nucleic acid and protein. Fe^{3+} acts as an electron acceptor and is a metal ion with an incomplete orbital. TPS has a conjugated π-electron system and contains electron-donating groups such as hydroxyl and carboxyl, which can coordinate with Fe^{3+} as an organic compound. The UV absorption capacity of the TPS-Fe(III) complex was stronger than that of TPS, signifying that TPS and Fe^{3+} can form a complex. The electron transfer transition band of the ligand in the ultraviolet region causes strong absorption. The carbonyl, carboxyl, and ester groups are the typical chromophores that produce absorption peaks in the UV–Vis region, whereas the hydroxyl and sulfhydryl groups are the common auxochrome. The chromophore and auxochrome in TPS are mainly the carboxyl and hydroxyl groups, respectively (Ma et al., 2013). The absorption of the complex in the ultraviolet region was higher than that of TPS. The results indicated that the carboxyl and hydroxyl groups may participate in the coordination reaction and change the absorption intensity of the ultraviolet light region.

3.7 Structural analysis of ^{1}H NMR

The structural characteristics of TPS and the TPS-Fe(III) complex were analysed through 1H NMR spectroscopy. As per ^{1}H NMR spectra, the NMR absorption peaks of the polysaccharide macromolecules were primarily distributed in the region with

a shift of δ3.5–5.5 ppm, which is the characteristic region of the polysaccharides signal. Figure 5A shows the ^{1}H NMR spectrum of TPS. The highly overlapping hydrogen signals in the δH3.22–4.12 ppm range can be designated as the C-2 to C-5 (or C-6) proton signals of the glycoside ring, whereas the hydrogen signal at δH4.3–5.5ppm represents the terminal stromal signal. According to the 1H NMR hydrogen spectra of the TPS-Fe(III) complex (Figure 5B), the displacement occurred between δ4.5 and 5.5 ppm, except for the strong resonance absorption peak of heavy water solvent near δ4.78 ppm, because no other clear resonance absorption peak was evident. This phenomenon was observed probably because the iron element is paramagnetic and can interfere with the magnetic environment near polysaccharides. This makes the relaxation time of other absorption peaks previously visible longer and spectrum peaks wider, thus forming the apparent phenomenon of reduced or invisible NMR absorption peaks (Hu et al., 2018).

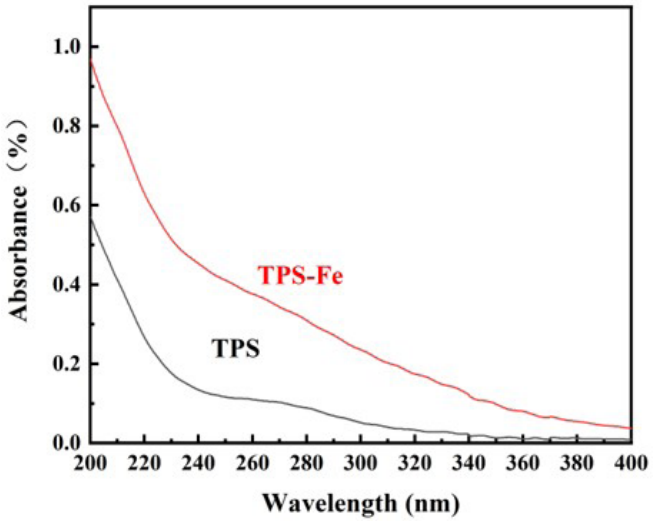

Figure 4. UV spectra fingerprint of TPS and the TPS-Fe(III) complex.

3.8 Morphology and elemental distribution of TPS-Fe(III)

Typical SEM micrographs of TPS and the TPS-Fe(III) complex are displayed in Figure 6. The surface of TPS (A) and TPS-Fe(III) complex (B) exhibited obvious changes in size and shape. Under the condition of 1000 times magnification, the TPS-Fe(III) complex exhibited a sheet shape (Zhang et al., 2019). Simultaneously, the EDS analysis indicated the presence of iron element in the TPS-Fe(III) complex. A clear iron signal was observed in the TPS-Fe(III) complex. The TPS did not contain iron; however, the iron content in the TPS-Fe(III) complex was 0.85%. The results showed that the synthesis conditions of the TPS-Fe(III) complex were feasible.

3.9 XRD crystal structure of the TPS-Fe(III) complex

Figure 7 depicts an XRD pattern. XRD analysis is used for the structural analysis of the internal distribution of atoms. X-rays passing through a crystalline material of a particular wavelength can be dispersed because the atoms or ions are arranged regularly within the crystal. The phase of the scattered X-rays is improved in some directions. Hence, specific diffraction phenomena correspond to the crystal structure. Both samples exhibited less crystallinity and lacked sharp crystallisation peaks. After the coordination reaction, the crystal morphology changed. XRD results of the TPS-Fe(III) complex exhibited different peak positions, signifying that the crystallinity of polysaccharides changed after incorporation of iron (Ghribi et al., 2015) . Collectively, iron was introduced into TPS, and the TPS-Fe(III) complex was successfully formed, as confirmed through XRD characterisation.

3.10 X-ray photoelectron spectroscopy

Figure 8 illustrates the XPS full-scan maps (A) and the Fe2p Scanning maps (B) of TPS and the TPS-Fe(III) complex. In the TPS sample, the characteristic peak of Fe was not found in the full-scan map and the XPS map of Fe2p, which indicated the lack of Fe in the sample. However, in the TPS-Fe(III) sample, the

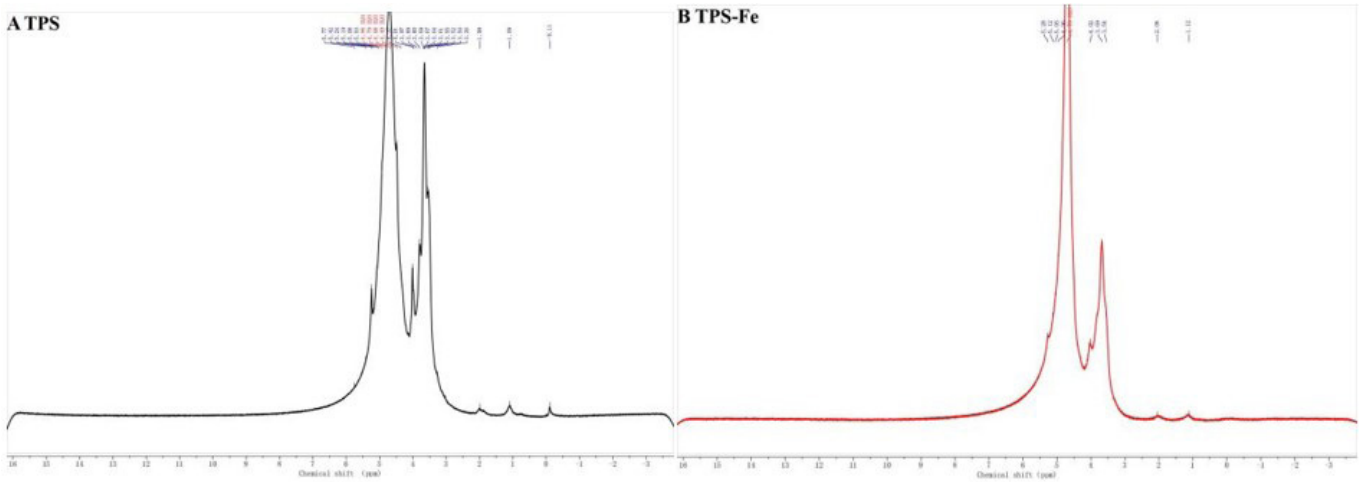

Figure 5. ^{1}H NMR spectra of TPS (A) and TPS-Fe(III) (B).

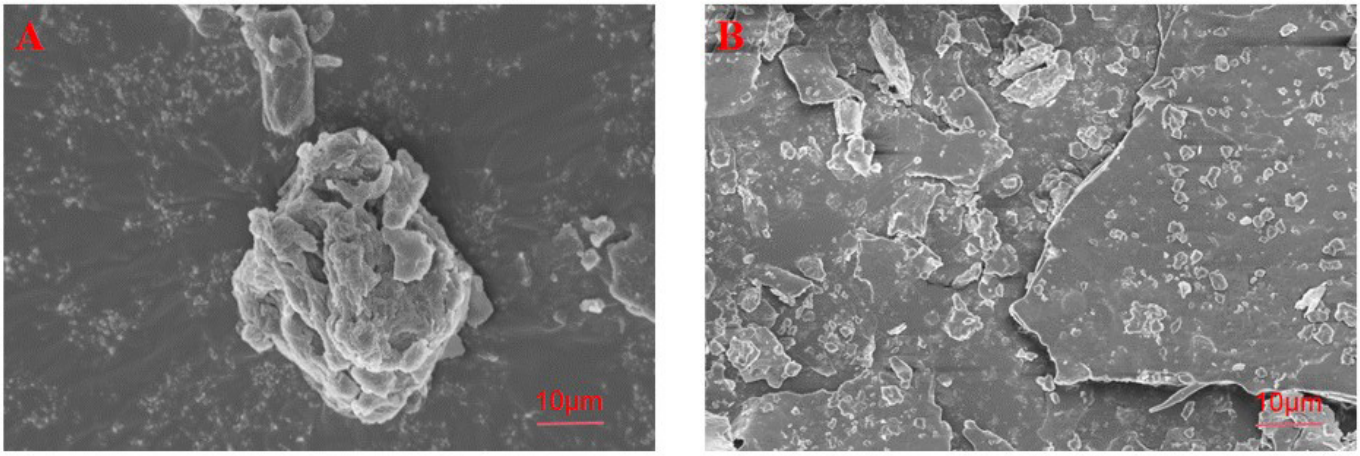

Figure 6. SEM images for TPS (A) and the TPS-Fe(III) complex (B).

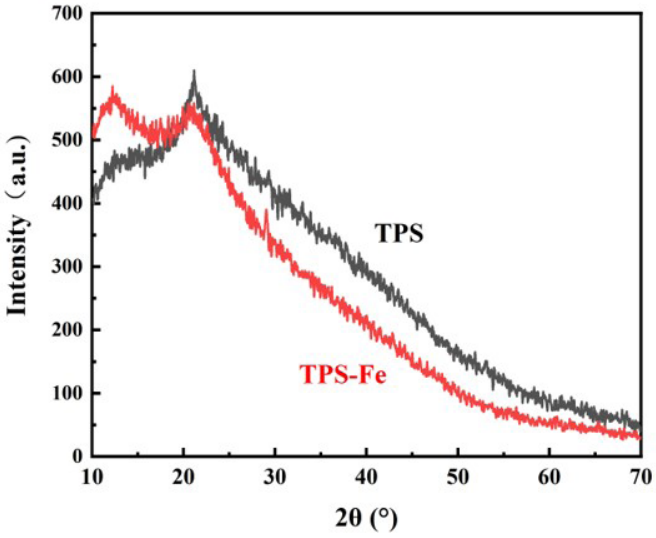

Figure 7. XRD diffraction spectra of TPS and the TPS-Fe(III) complex.

characteristic electron binding energy peaks of Fe were found in the XPS scanning spectra of Fe2p. It can be inferred that the Fe element successfully modifies the polysaccharides after the reaction (Gao et al., 2018; Wang et al., 2015).

3.11 AFM analysis

An atomic force microscope was used to examine the morphology of the TPS-Fe(III) complex. Chemical modifications can change the spatial structure of polysaccharides, thereby affecting its structure–activity relationship. The spatial structure or conformation of the polysaccharides plays a vital role in biological activity (Lu et al., 2016) . Figure 9 illustrates the topography images of TPS and the TPS-Fe(III) complex. The AFM image indicated that the particle size of the TPS-Fe(III) complex was smaller than that of TPS, and the distribution of TPS-Fe(III) was more uniform. This may be because the addition of iron is beneficial for optimising the disordered structure of polysaccharides, which causes aggregation of the sugar chain.

3.12 DPPH free radical scavenging experiment

DPPH can produce stable nitrogen-centred free radicals in the organic solvent methanol, which is dark purple and has a strong absorbance peak at 518 nm. The relationship is linear in a certain concentration range between the content of DPPH free radical and absorbance. The hydrogen supply is related to the scavenging activity of DPPH in the reaction system. When the activity of the DPPH radical is reduced at 518 nm, the colour of the sample changes, resulting in a decrease in absorbance. The scavenging activity of TPS and the TPS-Fe(III) complex at different concentrations was estimated using the aforementioned principle. As displayed in Figure 10, both TPS and the TPS-Fe(III) complex showed a certain degree of DPPH radical scavenging activity. With an increase in the concentration, the corresponding DPPH free radical scavenging rate gradually improved. At the 1.0 mg/mL concentration, the DPPH radical scavenging activities of TPS and the TPS-Fe(III) complex were 31.56% and 51.55%, respectively. The EC_{50} values of the DPPH radical scavenging activity of TPS and TPS-Fe(III) complex were 1.584 mg/mL and 0.970 mg/mL, respectively. The results indicated that the DPPH radical scavenging activity of TPS and the TPS-Fe(III) complex amplified with an increase in concentration, and both showed a certain degree of concentration dependence. The scavenging activity of the TPS-Fe(III) complex was higher than that of TPS in the concentration range of 0.0–1.0 mg/mL.

3.13 Hydroxyl radical scavenging experiment

Hydroxyl radical is an active substance of reactive oxygen that has a very strong oxidising ability. It can kill red blood cells, degrade DNA, cell membrane, and macromolecules, and cause great harm to human health. Thus, the removal of hydroxyl free radicals is one of the effective measures to prevent diseases. Here, we adopted the Fenton method to establish a reaction model, where Fe^{2+} can react with H_2O_2 to produce much short-lived hydroxyl radicals with high activity. In case of the addition of

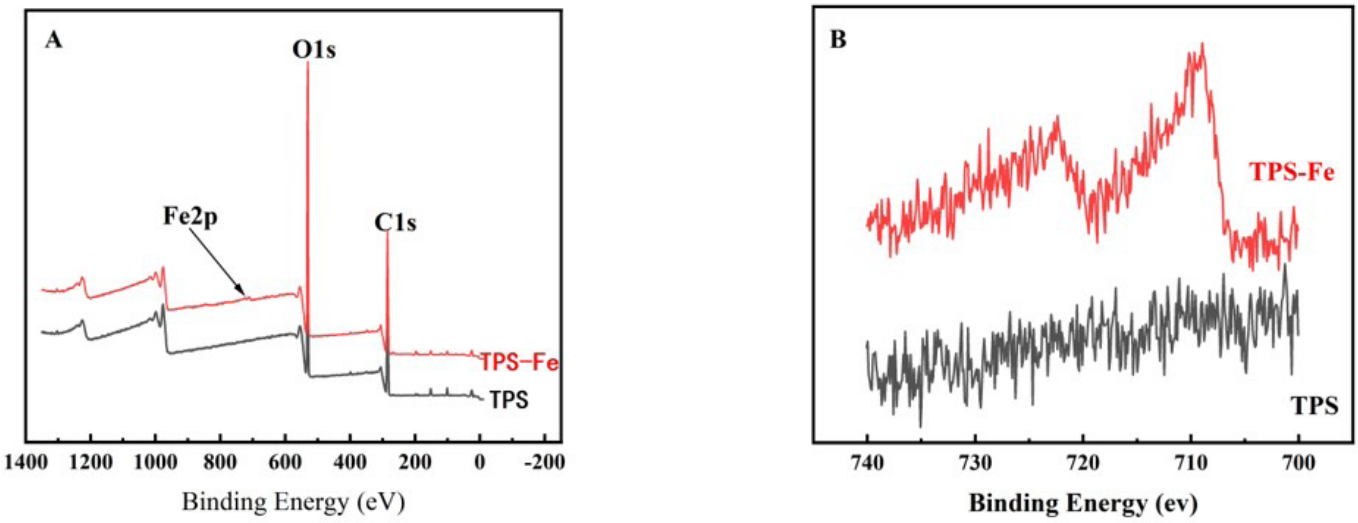

Figure 8 A: XPS full-scan maps of TPS and the TPS-Fe(III) complex; B: Fe2p scanning maps of TPS and the TPS-Fe(III) complex.

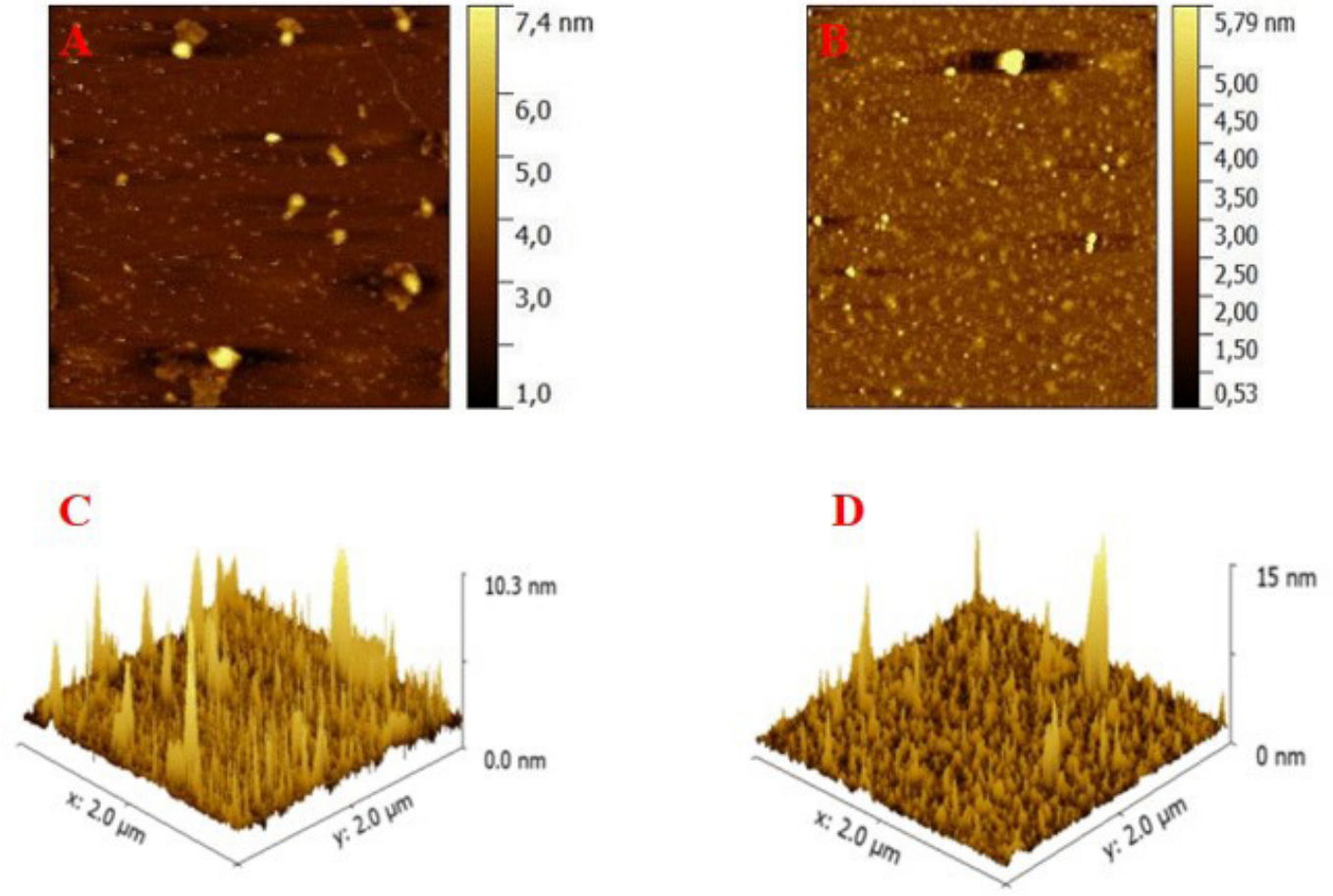

Figure 9. AFM topography images in the tapping mode. A: Topography image of TPS; B: Topography image of the TPS-Fe(III) complex; C: Height distribution of TPS; D: Height distribution of the TPS-Fe(III) complex.

excessive salicylic acid, the free radicals would attack the benzene ring of salicylic acid and generate 2, 3-dihydroxybenzoic acid, with a strong absorbance peak at 510 nm. When the sample has the antioxidant ability to scavenge hydroxyl radical, it can compete with salicylic acid and react with hydroxyl radical to absorb 2, 3-dihydroxybenzoic acid and decrease the absorbance

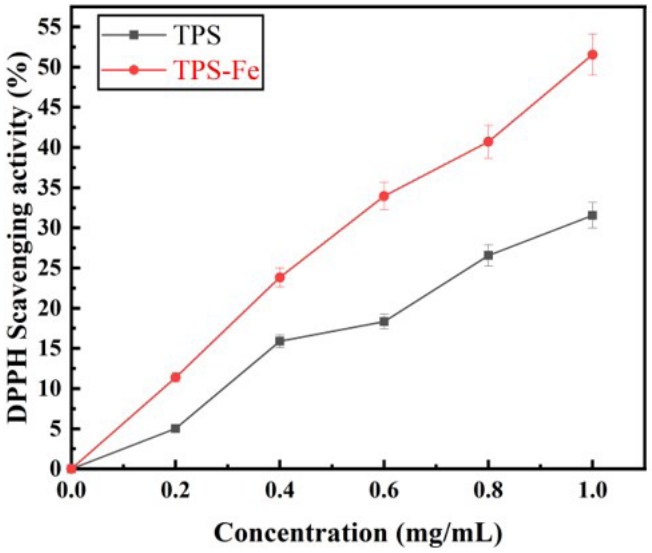

Figure 10. DPPH radical scavenging activity of TPS and the TPS-Fe(III) complex.

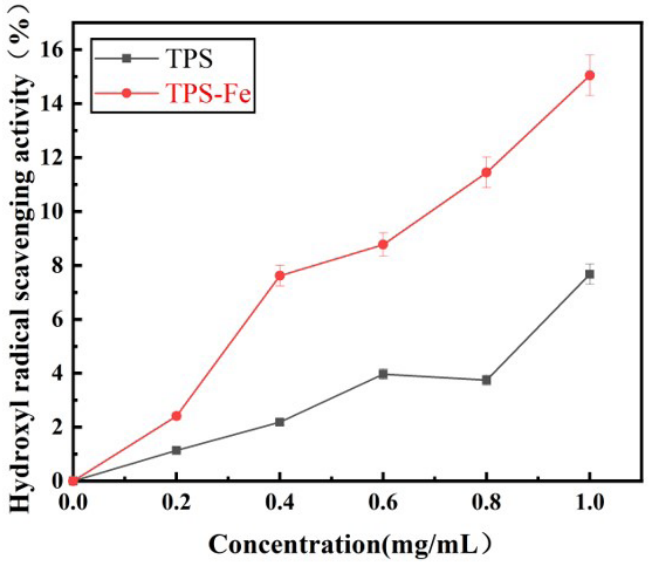

Figure 11. Hydroxyl radical scavenging activity of TPS and the TPS-Fe(III) complex.

at 510 nm. The hydroxyl radical scavenging activity of TPS and the TPS-Fe(III) complex is delineated in Figure 11. In the experiment, the concentration of the samples ranged from 0.0 mg/mL to 1.0 mg/mL. The hydroxyl radical scavenging activity of the samples increased with the increase in concentration and exhibited a certain degree of concentration dependence. In general, the TPS-Fe(III) complex has a higher hydroxyl radical scavenging ability than TPS. The scavenging activity of TPS and the TPS-Fe(III) complex was 7.67% and 15.04%, respectively, at 1.0 mg/mL concentration. The EC_{50} values of the hydroxyl radical scavenging activity of TPS and the TPS-Fe(III) complex were 6.515 mg/mL and 3.324 mg/mL, respectively.

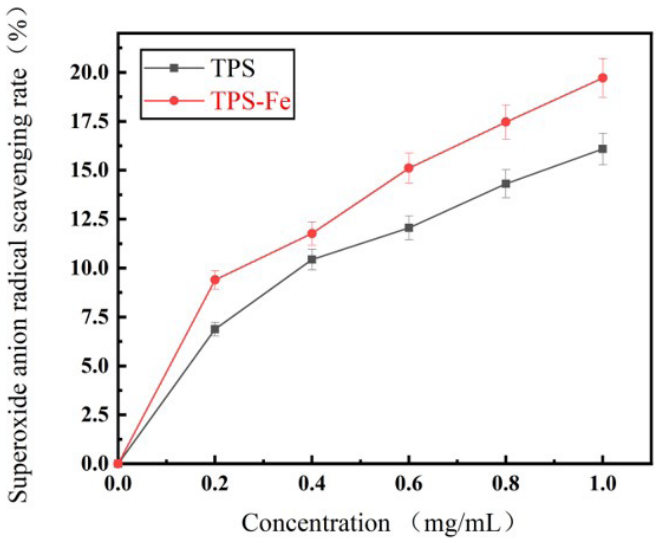

Figure 12. Superoxide anion radical scavenging activity of TPS and the TPS-Fe(III) complex.

3.14 Superoxide ion free radical scavenging experiment

Super oxygen ions produce a type of active oxygen free radicals in the human body that can cause serious damage such as body lipid peroxidation, skin disease, cardiovascular disease, and cancer and accelerate the body's ageing process. Superoxide dismutase can clear the superoxide anion radicals within the cell, and antioxidants can also be used to remove free radicals. The pyrogallol method is often used to spot the ability of antioxidants to scavenge superoxide free radicals; hence, the we adopted the pyrogallol oxidation method. The scavenging activity of superoxide root ion free radicals is outlined in Figure 12; as shown in the figure, the TPS-Fe(III) complex exhibited a stronger ability to scavenge free radicals than TPS. At 1.0 mg/mL, the scavenging rates of TPS and the TPS-Fe(III) complex were 16.08% and 19.72%, respectively. The EC_{50} values of the superoxide radical scavenging activity of TPS and the TPS-Fe(III) complex were 3.109 mg/mL and 2.536 mg/mL, respectively. The sample may react with pyrogallol or supply hydrogen to superoxide anion radicals and thus scavenge the free radicals. The results indicated that TPS and the TPS-Fe(III) complex possess a strong ability to inactivate superoxide anion radicals.

3.15 ABTS free radical scavenging experiment

In the form of 2,2-diazo-bis(3-ethyl-benzothiazole-6-sulfonic acid) diammonium salt, ABTS can react with $K_2S_2O_8$ to generate a stable, blue cationic radical and exhibits a clear absorption peak at 734 nm. Hence, its concentration can be determined by detecting the absorbance at 734 nm. If the reaction system becomes shallow, and the absorbance at 734 nm decreases when a sample is added to the ABTS free radical solution, the substance has free radical scavenging activity and is an antioxidant. According to the aforementioned principles, the ABTS scavenging activity of TPS and the TPS-Fe(III) complex at different concentrations was estimated; the results are displayed in Figure 13. The TPS-Fe(III)

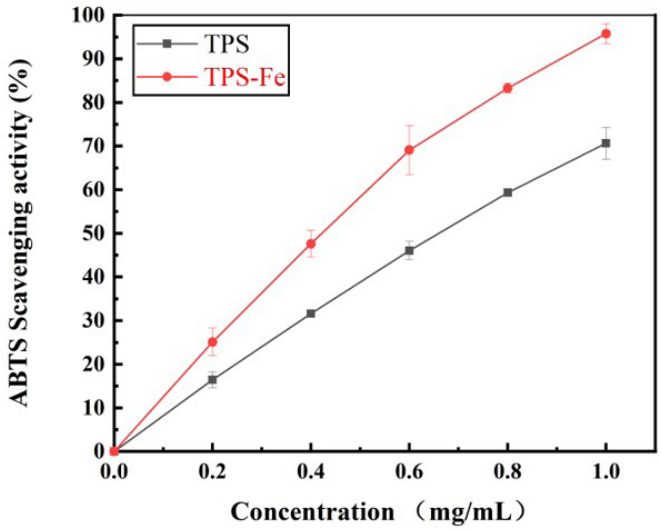

Figure 13. ABTS radical scavenging activity of TPS and the TPS-Fe(III) complex.

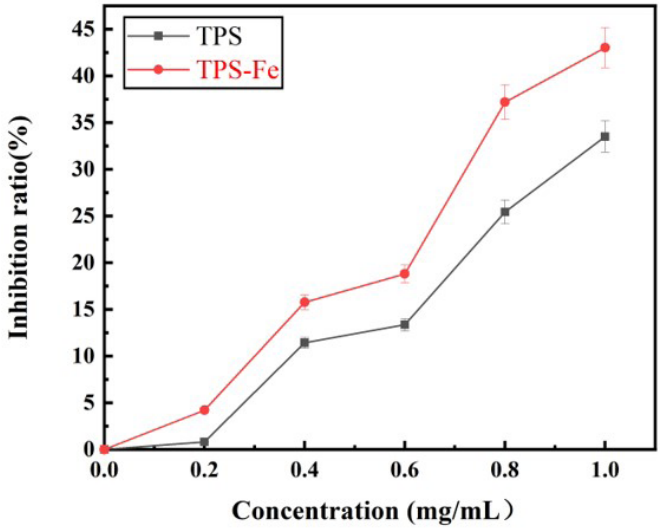

Figure 14. Lipid peroxidation inhibition activity of TPS and the TPS-Fe(III) complex.

complex displayed a clear ABTS radical scavenging activity of 95.76% at the concentration of 1.0 mg/mL. Though the ABTS free radical scavenging activity of TPS was lower than that of TPS-Fe (III), it still showed certain activity. The maximum ABTS free radical scavenging activity of TPS reached 70.62% at 1.0 mg/mL. The EC_{50} values of the ABTS radical scavenging activity of TPS and the TPS-Fe(III) complex 0.708 mg/mL and 0.522 mg/mL, respectively. The ABTS radical scavenging activity of TPS and the TPS-Fe(III) complex exhibited some degree of concentration dependence.

3.16 Liver lipid peroxidation inhibition activity test

Malondialdehyde (MDA) is a normally used lipid peroxidation index. Under acidic and high temperature conditions, it can react with TBA to form the reddish-brown trimethanol-3,5,5-trimethyloxazole-2,4-dione, which exhibits the maximum absorption wavelength of 532 nm. The mouse liver homogenate containing Fe^{2+} and H_2O_2 can effectively increase free radical expression and cause liver peroxidation, thereby increasing the production of MDA. Antioxidants can also prevent the expression of free radicals. Figure 14 depicts the ability of the sample to inhibit MDA production in the Fe^{2+} and H_2O_2 system-induced live homogenate of healthy mice. The inhibition rates of TPS and the TPS-Fe(III) complex were 33.51% and 43.02%, respectively, at 1.0 mg/mL, whereas the EC_{50} values of TPS and the TPS-Fe(III) complex were 1.492 mg/mL and 1.162 mg/mL, respectively.

4 Conclusion

This study designed and characterised the TPS-Fe(III) complex that was prepared by combining TPS with Fe. The results indicated successful complexation of iron into the Qingzhuan Dark Tea polysaccharides, and the as-prepared TPS-Fe(III) was a stable thermal polysaccharide with a compact structure. The TPS-Fe(III) complex is a brown powder with the Fe content of 0.89%. The spectral data indicated that the Fe ion in the TPS-Fe(III) complex bound to the binding site in TPS. Hence, a spatially separated iron centre is formed on the main chain of polysaccharides. The FT-IR, UV–Vis, and XRD spectra of TPS were different from those of the TPS-Fe(III) complex, which indicated that their structures are diverse. Furthermore, the structural analysis showed that the polysaccharide ligands surround the iron in the core. The antioxidant activity of TPS and the TPS-Fe(III) complex of Qingzhuan Dark Tea was determined on the basis of the scavenging effects on DPPH radical, hydroxyl radical, ABTS radical, and superoxide anion radical and the inhibition effect on lipid peroxidation. In particular, the TPS-Fe(III) complex exhibited stronger free radical scavenging ability than TPS, although this ability was concentration-dependent for both samples. The results showed that TPS-Fe(III) could form organic iron supplements with a strong antioxidant activity. Simultaneously, it provides a scientific basis for further development and utilisation of TPS. However, the complex relationship between the structural characteristics of TPS-Fe(III) and its antioxidant activity may be affected by different combinations of factors, and the exploration of the mechanism of TPS-Fe(III) antioxidant activity in Qingzhuan Dark Tea warrants further studies.

Ethical approval

This article does not contain any studies with human participants or animals performed by any of the authors.

Conflict of interest

The authors declare that they have no conflicts of interest.

Acknowledgements

We thank Dr. Tao Chen and Dr. Juntao Wang for their assistance with the experiments and imaging. This work was supported by the Key Scientific Instrument Special Project of China's National Natural Science Foundation (Project No. 81727805), Hubei Provincial Department of Education

scientific Research Programme (B2019159), Doctor start fund project (BK201803,BK202201), and Hundred schools and hundred counties project (BXLBX0794,BXLBX0795),Young and middle-aged talents Project (Q20212803),Xianning key special project for scientific and technological research and development(2021SFYF003).

References

Abualhasan, M., Dwaikat, S., Ataya, R., Ali, A., & Al-Atrash, M. (2021). Quality evaluation of iron-containing food supplements in the Palestinian market. *Food Science and Technology*, 41(Suppl. 2), 785-790. http://dx.doi.org/10.1590/fst.01621.

Akram, K., Shahbaz, H. M., Kim, G.-R., Farooq, U., & Kwon, J.-H. (2017). Improved extraction and quality characterization of water-soluble polysaccharide from gamma-irradiated lentinus edodes. *Journal of Food Science*, 82(2), 296-303. http://dx.doi.org/10.1111/1750-3841.13590. PMid:28152202.

Byun, N., Cho, J., & Yim, S. (2021). Correlation between antioxidant activity and anti-wrinkle effect of ethanol extracts of Sanguisorba Officinalis L. *Food Science and Technology*, 41(Suppl. 2), 791-798. http://dx.doi.org/10.1590/fst.10921.

Dong, Y.-R., Cheng, S.-J., Qi, G.-H., Yang, Z.-P., Yin, S.-Y., & Chen, G.-T. (2017). Corrigendum to "Antimicrobial and antioxidant activities of Flammulina velutipes polysacchrides and polysacchride-iron(III) complex". *Carbohydrate Polymers*, 165, 470. http://dx.doi.org/10.1016/j.carbpol.2017.02.090. PMid:28363574.

Feng, G., & Zhang, X.-F. (2020). Production of a codonopsis polysaccharide iron complex and evaluation of its properties. *International Journal of Biological Macromolecules*, 162, 1227-1240. http://dx.doi.org/10.1016/j.ijbiomac.2020.06.210. PMid:32615228.

Feng, L., Liu, P., Zheng, P., Zhang, L., Zhou, J., Gong, Z., Yu, Y., Gao, S., Zheng, L., Wang, X., & Wan, X. (2020). Chemical profile changes during pile fermentation of Qingzhuan tea affect inhibition of α-amylase and lipase. *Scientific Reports*, 10(1), 3489. http://dx.doi.org/10.1038/s41598-020-60265-2. PMid:32103067.

Gao, W., Huang, Y., He, R., & Zeng, X.-A. (2018). Synthesis and characterization of a new soluble soybean polysaccharide-iron(III) complex using ion exchange column. *International Journal of Biological Macromolecules*, 108, 1242-1247. http://dx.doi.org/10.1016/j.ijbiomac.2017.11.038. PMid:29128590.

Gao, Y., Cao, Z., Zhou, F., Zhao, Y., Tang, L., & Zhang, H. (2021). Association between tea drinking and endometrial cancer risk: a meta-analysis. *Food Science and Technology*. Ahead of print. http://dx.doi.org/10.1590/fst.90021.

Ghribi, M., Abir, S., Assaâd, M. G., Ines, B., Christophe, D., Sabine, A., Hamadi, B., & Ali, B. (2015). Structural, functional, and ACE inhibitory properties of water-soluble polysaccharides from chickpea flours. *International Journal of Biological Macromolecules*, 75, 276-282. http://dx.doi.org/10.1016/j.ijbiomac.2015.01.037. PMid:25643994.

Guo, L., Ding, W., & Meng, F. (2014). Fabrication and *in vitro* evaluation of folate-modified iron ferrite nanoparticles with high doxorubicin loading for receptors-magnetic-guided drug delivery. *Nano*, 09(2), 1450021. http://dx.doi.org/10.1142/S1793292014500210.

Hu, J., Gao, J., Zhao, Z., & Yang, Z. (2021). Response surface optimization of polysaccharide extraction from Galla Chinensis and determination of its antioxidant activity in vitro. *Food Science and Technology*, 41(1), 188-194. http://dx.doi.org/10.1590/fst.38619.

Hu, X., Wang, Y., Zhang, L., Xu, M., Zhang, J., & Dong, W. (2018). Magnetic field-driven drug release from modified iron oxide-integrated polysaccharide hydrogel. *International Journal of Biological Macromolecules*, 108, 558-567. http://dx.doi.org/10.1016/j.ijbiomac.2017.12.018. PMid:29233710.

Iwansyah, A. C., Desnilasari, D., Agustina, W., Pramesti, D., Indriati, A., Mayasti, N. K. I., Andriana, Y., & Kormin, F. B. (2021). Evaluation on the physicochemical properties and mineral contents of Averrhoa bilimbi L. leaves dried extract and its antioxidant and antibacterial capacities. *Food Science and Technology*, 41(4), 987-992. http://dx.doi.org/10.1590/fst.15420.

Li, W., Wang, Y., Wei, H., Zhang, Y., Guo, Z., Qiu, Y., Wen, L., & Xie, Z. (2020). Structural characterization of Lanzhou lily (Lilium davidii var. unicolor) polysaccharides and determination of their associated antioxidant activity. *Journal of the Science of Food and Agriculture*, 100(15), 5603-5616. http://dx.doi.org/10.1002/jsfa.10613. PMid:32608519.

Liu, S., Yu, Z., Zhu, H., Zhang, W., & Chen, Y. (2016). In vitro α-glucosidase inhibitory activity of isolated fractions from water extract of Qingzhuan dark tea. *BMC Complementary and Alternative Medicine*, 16(1), 378. http://dx.doi.org/10.1186/s12906-016-1361-0. PMid:27681250.

Liu, T., Liu, T., Liu, H., Fan, H., Chen, B., Wang, D., Zhang, Y., & Sun, F. (2019). Preparation and characterization of a novel polysaccharide-iron(iii) complex in auricularia auricula potentially used as an iron supplement. *BioMed Research International*, 2019, 6416941. http://dx.doi.org/10.1155/2019/6416941. PMid:31309110.

Liu, Y., & Li, S. (2021). Extraction optimization and antioxidant activity of Phyllanthus urinaria polysaccharides. *Food Science and Technology*, 41(Suppl. 1), 91-97. http://dx.doi.org/10.1590/fst.11320.

Lu, Q., Xu, L., Meng, Y., Liu, Y., Li, J., Zu, Y., & Zhu, M. (2016). Preparation and characterization of a novel Astragalus membranaceus polysaccharide-iron (III) complex. *International Journal of Biological Macromolecules*, 93(Pt A), 208-216. http://dx.doi.org/10.1016/j.ijbiomac.2016.08.049. PMid:27544435.

Ma, L., Chen, H., Zhu, W., & Wang, Z. (2013). Effect of different drying methods on physicochemical properties and antioxidant activities of polysaccharides extracted from mushroom Inonotus obliquus. *Food Research International*, 50(2), 633-640. http://dx.doi.org/10.1016/j.foodres.2011.05.005.

Raja, K. B., Jafri, S. E., Dickson, D., Acebròn, A., Cremonesi, P., Fossati, G., & Simpson, R. J. (2000). Involvement of iron (ferric) reduction in the iron absorption mechanism of a trivalent iron-protein complex (iron protein succinylate). *Pharmacology & Toxicology*, 87(3), 108-115. http://dx.doi.org/10.1034/j.1600-0773.2000.pto870302.x. PMid:11068850.

Tveden-Nyborg, P., Bergmann, T. K., Jessen, N., Simonsen, U., & Lykkesfeldt, J. (2021). BCPT policy for experimental and clinical studies. *Basic & Clinical Pharmacology & Toxicology*, 128(1), 4-8. http://dx.doi.org/10.1111/bcpt.13492. PMid:32955760.

Wang, J., Chen, H., Wang, Y., & Xing, L. (2015). Synthesis and characterization of a new Inonotus obliquus polysaccharide-iron(III) complex. *International Journal of Biological Macromolecules*, 75, 210-217. http://dx.doi.org/10.1016/j.ijbiomac.2015.01.041. PMid:25643995.

Wang, Y., Peng, Y., Wei, X., Yang, Z., Xiao, J., & Jin, Z. (2021). Corrigendum to "Sulfation of tea polysaccharides: Synthesis, characterization and hypoglycemic activity". *International Journal of Biological Macromolecules*, 189, 1043-1044. http://dx.doi.org/10.1016/j.ijbiomac.2021.08.192. PMid:34538667.

Yang, L., Liu, H., Zhao, R., Li, C., Gu, W., & Jin, T. (2020). Fluorescence enhancement method for palmatine extraction by SWMONTs. *Journal of Coordination Chemistry*, 73(4), 579-592. http://dx.doi.org/10.1080/00958972.2020.1742330.

Yang, X., Huang, M., Qin, C., Lv, B., Mao, Q., & Liu, Z. (2017). Structural characterization and evaluation of the antioxidant activities of polysaccharides extracted from Qingzhuan brick tea. *International Journal of Biological Macromolecules*, 101, 768-775. http://dx.doi.org/10.1016/j.ijbiomac.2017.03.189. PMid:28373046.

Yao, Q., Lin, Q., Yan, S., Huang, M., & Chen, L. (2021). Dietary risk assessment of fluoride, lead, chromium, and cadmium through consumption of Tieguanyin tea and white tea. *Food Science and Technology*, 41(3), 782-789. http://dx.doi.org/10.1590/fst.69220.

Zhang, J., Chen, C., & Fu, X. (2019). Fructus mori L. polysaccharide-iron chelates formed by self-embedding with iron(iii) as the core exhibit good antioxidant activity. *Food & Function*, 10(6), 3150-3160. http://dx.doi.org/10.1039/C9FO00540D. PMid:31166348.

Zhang, X., Zhang, X., Gu, S., Pan, L., Sun, H., Gong, E., Zhu, Z., Wen, T., Daba, G. M., & Elkhateeb, W. A. (2021). Structure analysis and antioxidant activity of polysaccharide-iron (III) from Cordyceps militaris mycelia. *International Journal of Biological Macromolecules*, 178, 170-179. http://dx.doi.org/10.1016/j.ijbiomac.2021.02.163. PMid:33639188.